# Anatomically realistic aortic dissection simulator as a potential training tool for point-of-care ultrasound

Mutiah Rahmah[1], Rania Hussien Al-Ashwal[2], Maheza Irna Mohamad Salim[2], Yan Tung Lam[1], Yuan Wen Hau[3]

[1] Department of Biomedical Engineering and Health Sciences, Faculty of Electrical Engineering, Universiti Teknologi Malaysia, Skudai, Malaysia
[2] Advanced Diagnostic and Progressive Human Care research Group, Department of Biomedical Engineering and Health Sciences, Faculty of Electrical Engineering, Universiti Teknologi Malaysia, Skudai, Malaysia
[3] IJN-UTM Cardiovascular Engineering Centre, Department of Biomedical Engineering and Health Sciences, Faculty of Electrical Engineering, Universiti Teknologi Malaysia, Skudai, Malaysia

Corresponding author: Rania Hussien Al-Ashwal; e-mail: rania@utm.my

DOI: 10.15557/JoU.2024.0002

Abstract

**Aim:** Simulators for aortic dissection diagnosis are limited by complex anatomy influencing the accuracy of point-of-care ultrasound for diagnosing aortic dissection. Therefore, this study aimed to create a healthy ascending aorta and class DeBakey, type II aortic dissection simulator as a potential point-of-care ultrasound training model. **Material and methods:** 3D mould simulators were created based on computed tomography images of one healthy and one DeBakey type II aortic dissection patient. In the next step, two polyvinyl alcohol-based and two silicone-based simulators were synthesised. **Results:** The results of the scanning electron microscope assessment showed an aortic dissection simulator's surface with disorganised surface texture and higher root mean square (RMS or Rq) value than the healthy model of polyvinyl alcohol ($Rq_{AD}$ = 20.28 > $Rq_{AAo}$ = 10.26) and silicone ($Rq_{AD}$ = 33.8 > $Rq_{AAo}$ = 23.07). The ultrasound assessment of diameter aortic dissection showed higher than the healthy ascending aorta in polyvinyl alcohol ($d_{AD}$ = 28.2 mm > $d_{AAo}$ = 20.2 mm) and Si ($d_{AD}$ = 31.0 mm > $d_{AAo}$ = 22.4 mm), while the wall thickness of aortic dissection showed thinner than the healthy aorta in polyvinyl alcohol, which is comparable with the actual aorta measurement. The intimal flap of aortic dissection was able to replicate and showed a false lumen in the ultrasound images. The flap was measured quantitatively, indicating that the intimal flap was hyperechoic. **Conclusions:** The simulators were able to replicate the surface morphology and echogenicity of the intimal flap, which is a linear hyperechoic area representing the separation of the aorta wall.

## Introduction

Aortic dissection causes propagated damage (proximally or distally) due to blood entering the intima-media space[1]. The mortality associated with aortic dissection (AD) is high; in Malaysia, the number of cases of aortic aneurysm which can cause AD is predicted to reach 15,299 cases among the total population of 23 million people[2]. The two most common anatomic classification systems for AD are the Stanford and the DeBakey. The Stanford system is further classified into two affected areas, type A is in the ascending aorta, which is the case for most patients, but there are exceptions, as in type B, which involves the descending area. The DeBakey classification is divided into type I, type II, and type III. Type I dissection is affecting the entire aorta, type II involves the ascending area only, while type III is usually found in the descending

area, excluding the ascending and aortic arch[3]. Stanford type A and DeBakey type II, which include ascending areas in the affected area, are associated with higher mortality rates than type B. Symptoms such as chest pain have been reported in a higher percentage (85%) of type A than type B (67%) patients, but hypertension in type A patients' condition occurs in fewer cases than type B. It causes AD patients type A to increasingly be transferred to the aortic specialist department for further assessment to determine emergent surgery needs[4].

Several types of imaging modalities are employed to diagnose AD, with US typically used in emergency departments because it is non-invasive and can diagnose disorders in a short time[5]. The utility of ultrasound (US) encompasses a wide range of medical conditions involving the cardiovascular, respiratory, and vascular systems.

US also shows high accuracy for the detection of aortic aneurysm (100%) if the diameter size is 3 cm[6]. The advantage of US to utilise as a point-of-care ultrasound (PoCUS) is that it is easy for handheld devices, easy to perform the assessment, and not time-intensive[7].

Physicians lack practical experience and have fewer opportunities to acquire expertise in clinical settings directly in patients due to safety reasons[8]. Therefore, nowadays, simulators are used for training and education purposes[9]. The training simulation method can produce clinical scenarios, help physicians to encounter and respond to abnormal conditions, and reduce the potential for provider deficiencies during the assessment[8]. Training simulators rely on 3D printing technologies for rapidly prototyping and converting digital objects into physical objects which were applied in this study to extrude a mould[10]. In medical and clinical research, tissue mimicking materials (TMM) are usually used, including biopolymers (agarose, gelatin, and gellan gum) and synthesised polymers (polyvinyl alcohol (PVA), silicone, and polyvinyl chloride). The advantages of PVA include non-toxicity, biocompatibility, and biodegradability[11]. The purpose of aluminium oxide ($Al_2O_3$) in tissue mimicking is to act as a scatterer during ultrasound assessments[12]. Glycerol ($C_3H_8O_3$) serves as a plasticiser and simulates better mechanical properties[13]. Silicone owes its benefits to durability, stability over time, and strongly hydrophobic properties. Additive materials such as graphite have roles as a scattering agent, thinner to reduce viscosity, and slacker to provide a human tissue-like self-sealing property[14].

The present study aimed to create an ascending aorta (AAo) and DeBakey type II AD simulator synthesised by polyvinyl alcohol (PVA) and silicone (Si), and study its surface morphology and ultrasound features (diameter, wall thickness, and echogenicity) as a potential PoCUS training model.

## Methodology

### Materials and equipment

The chemical materials used included PVA with a molecular weight of 89,000–98,000 and 99+% hydrolyzed (Sigma-Aldrich), aluminium oxide ($Al_2O_3$) (Sigma-Aldrich), glycerol (QRec), silicone eco flex 00-10 (Smooth-On), slacker (Smooth-On), thinner (Smooth-On), graphite (Sigma-Aldrich), and agarose (Promega). The equipment utilised included a 3D printer machine (ender3pro), TM3000 TableTop SEM (Hitachi), and ultrasound Toshiba Aplio 300. The software used included Blender, Cura, IBM SPSS statistic 27, and ImageJ.

### Mould extrusion

The 3D image of healthy AAo and AD was acquired from an anonymous patient who was examined through CT scan provided by open source in *embodi3d.com/files/file/55961-aortic-arch/* for healthy AAo and *3d.nih.gov/entries/3DPX-005015* for AD in the stereolithography (STL) format, and then imported to Blender software to create the mould. The 3D design was split into the sagittal plane, with three main parts for each AAo and AD design, including the medial side, the core, and the lateral side. Two cubes were added, and the 3D image of the aorta was divided into half. Next, the size was modified to make sure that the core of the aorta was precisely in the middle of the mould. The complete 3D design of the mould boxes in the STL format was imported to the Cura software for slicing purposes, as shown in Fig. 1. The layer and the thickness of the filament were set at 0.1 mm and 0.8 mm, and the estimation time of the 3D printing process took approximately four to six hours for each part of the mould.

### Simulator fabrication

The first simulator of PVA composition was made up of 5% (2.5 g) and then dissolved in 50 mL of distilled water. Aluminium oxide (2%) and glycerol (12%) were also added to the PVA solution[11]. The mixed solution was then poured into the mould and solidified by using a freeze-thaw process. The freeze-thaw cycle was done by putting the mould into the freezer with a temperature -20°C for 12 hours and continuing to thaw in the room temperature for 12 hours. Then, the procedure was repeated for three cycles, which made up a total of 72 hours for the whole process[12]. The second solution was composed of part A and part B of silicone in a 1:1 ratio. Then, 53% of part A + part B silicone, 15% thinner and 7% of slacker was added to reduce the viscosity of the silicone and as the property of self-sealing process[14]. To enhance the echogenicity during US evaluation, 5% graphite was added as well. The solution was allowed to solidify at room temperature after mixing homogeneously. The demoulding process of the simulator was done manually to remove the simulator from the mould. To evaluate the simulator by US, a low-fidelity agar-based simulator was fabricated. A low-fidelity simulator was prepared by using distilled water (250 mL) and agarose (1%), then stirred for 30 minutes at 180°C until it completely dissolved. The agarose was allowed to cool down for three to five minutes before being poured into the container containing the simulators in order to prevent the melting of the PVA simulator. Finally, the agarose was allowed to solidify for an hour, and the simulator was ready for further testing.

### Characterisation of simulators

The characteristics studied included morphology (surface roughness and 3D plot surface) and ultrasound features (diameter, wall thickness, and echogenicity measurement). The SEM test was conducted using a TM3000 TableTop system to evaluate the surface morphology of the simulators. The sample was prepared by cutting the healthy AAo and the AD simulator into 1 cm × 1 cm pieces with a thickness of not more than 5 mm at the ascending part, which was the area of interest. The SEM magnification was set to 100×, as a standardisation from the previous study, to allow for an ideal comparison between the results of this study[15]. The samples were then coated with gold sputter to improve image quality.

Surface roughness was evaluated using imageJ, based on the SEM images. The roughness parameters were calculated using the root mean square (RMS), with (Rq) obtained from Fiji ImageJ and evaluated using the SurfCharj tools available in the windows menu. The images were converted to the 32-bit format and then sharpened to improve clarity. The data was analysed with the SurfCharJ tools from the plugins window[16]. The RMS value was compared between the healthy AAo and AD for the purpose of quantitative analysis. The 3D surface plot was measured through a plugin in the windows of imageJ menu to analyse the intensity of light from a surface plot of each pixel in the SEM images[17]. The surface plot profile in the menu shows the grey value of each pixel and the raw data used to analyse the variance by IBM SPSS statistic 27.
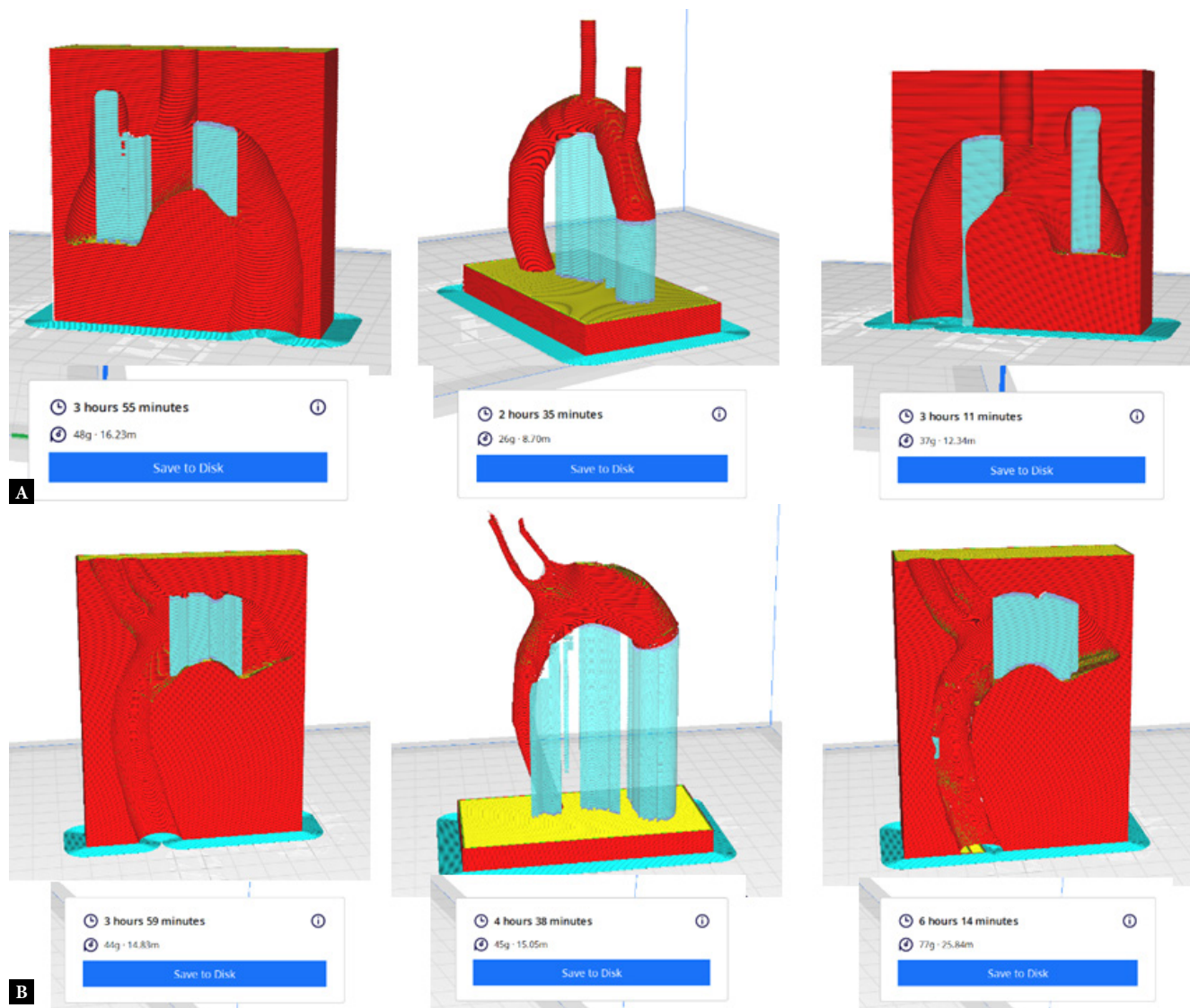
**Fig. 1.** *Final design of the mould in Cura software after the slicing process; the hours indicate the time estimation for completing the printing process and the weight mass (g) for the required filament.* **A.** *3D design of the healthy aorta mould.* **B.** *3D design of the aortic dissection mould*

The simulators were assessed by using a phased-array cardiac transducer type PST-65 AT (6.5 MHz) from the Toshiba Aplio 300 ultrasound system. The probe was put above the low-fidelity simulator and started with the transverse and long-axis view assessment. The image was freeze-captured in the transverse view to visualise the aortic wall, and the distance between the inner and outer walls of the aorta was used to calculate the thickness ($t$) of the aortic wall and measure the diameter ($d$) using the calliper button in the menu table. The probe was set to the transverse and long-view to check the intimal flap in the AD simulator. The freeze-captured B-mode image of the AD sim in the transverse view was then used to measure the echogenicity between the intimal flap and false lumen. The echogenicity calculation used imageJ to calculate the average grey of the intimal flap ($\mu_{IF}$) and the echogenicity index of the false lumen ($EI_{FL}$) in the dissected area of the AD simulator. The two areas of interest (intimal flap and false lumen) were selected using the polygon section in the command window of imageJ. Then the analyze menu was clicked to get the measurement, and the result of the mean grey value section appeared. The results of $\mu_{IF}$ and $EI_{FL}$ were then analysed using Fisher's exact test to determine any significant difference between the intimal flap and false lumen between the PVA and Si. A $p$ value less than 0.05 was considered as statistically significant.

## Result

### Physical description of the simulator

The simulator synthesised by PVA appeared transparent, and white crystalline precipitate of $Al_2O_3$ was observed (Fig. 2) on the wall of the healthy and AD's and also in the region of the flap. The rough surface on the ascending area of AD was visible due to the design of the mould.

In addition, the synthesised Si was black in colour due to the addition of graphite (Fig. 3). The Si simulator had a more precise structure
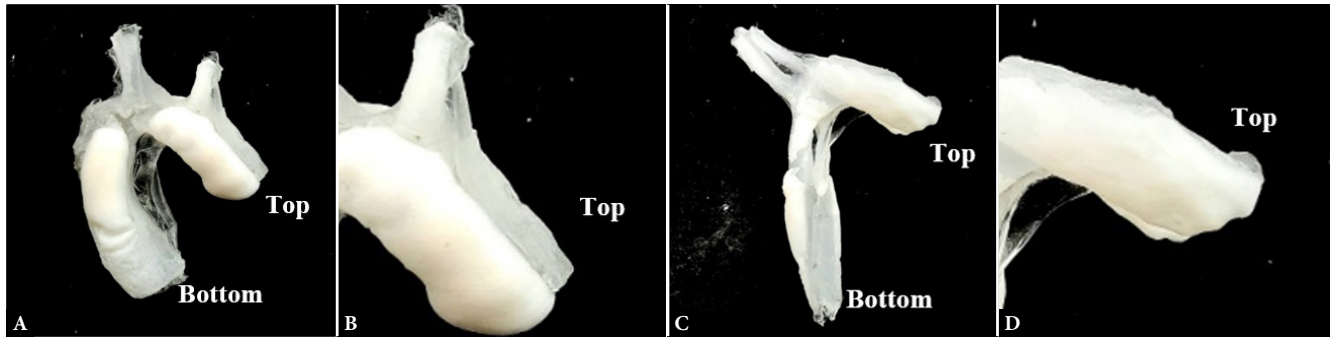
**Fig. 2.** *Synthesised simulator based on PVA.* **A.** *Healthy aorta simulator from top view* **B.** *Ascending aorta of the healthy aorta (point of interest)* **C.** *Aortic dissection simulator from top view* **D.** *Ascending aortic dissection (point of interest)*
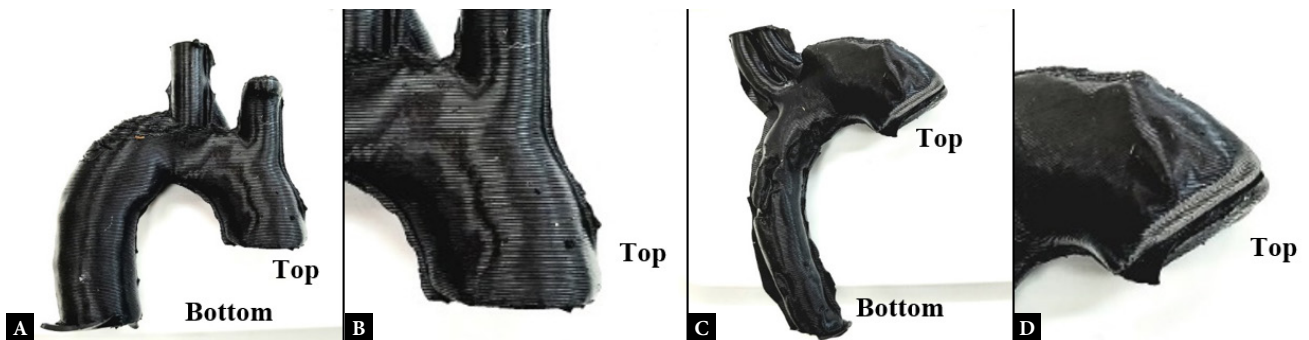


**Fig. 3.** *Synthesised simulator based on silicone.* **A.** *Healthy aorta simulator from top view* **B.** *Ascending aorta of the healthy aorta (point of interest)* **C.** *Aortic dissection simulator from top view* **D.** *Ascending aortic dissection (point of interest)*

than the PVA simulator due to the higher density of silicone, which makes it easier to mimic the detailed shape of the mould.

## Morphology analysis

The results of the SEM test in Tab. 1 show the differences between the AAo of the healthy aorta and the dissected area. The healthy aorta simulator synthesised by both PVA and Si showed a uniform line on the surface of the ascending area. The abnormal condition in the dissect area of both synthesised simulators was disorganised surface structure. The SEM image of an actual aorta was used as a reference (healthy AAo from Pasta *et al.* and AD from Schimitto, *et al.*) for the comparison between synthesised simulators and the actual aorta as shown in Tab. 1[18,19].

The RMS result of the healthy AAo simulator synthesised by PVA was $Rq_{AAo} = 10.26$ and in the aortic dissection simulator $Rq_{AD} = 20.28$. Besides, the healthy AAo simulator synthesised by Si yielded the result of $Rq_{AAo} = 23.07$, and in the AD simulator $Rq_{AD} = 33.8$. The actual organ of SEM images was also measured, and the results show $Rq_{AAo} = 13.11$ and $Rq_{AD} = 38.83$ in Tab. 2.

The 3D surface plot of SEM images shown in Tab. 3 consists of pixels or xyz-triples. The uniform line of the sharpening shape in the 3D plot of healthy AAo is consistently similar between the simulators and the actual aorta. The standard deviation was calculated, showing a small range between the AAo simulators $\sigma = 2.04$–$2.14$ and the actual AAo $\sigma = 0.92$. In addition, the AD surface showed higher dull shape and disorganised structure, as shown by the standard deviation results of simulators $\sigma = 5.35$–$9.59$ and the actual AAo $\sigma = 13.68$.
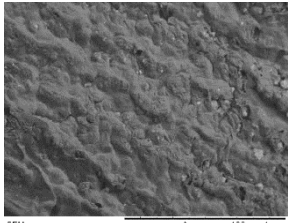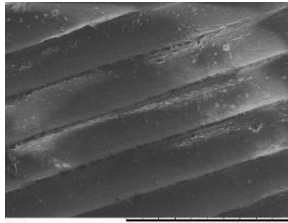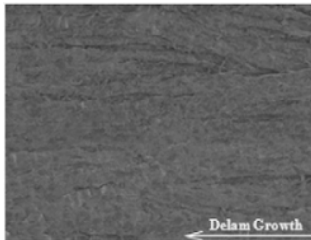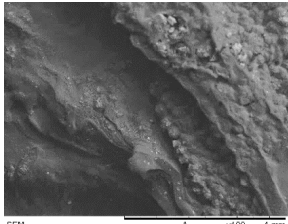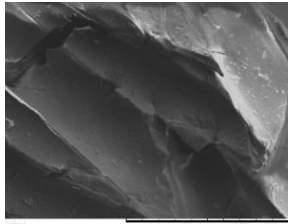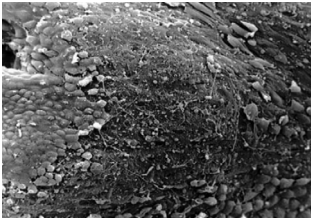
The surface plot shows the variance ($\sigma^2$) of the healthy AAo and AD, and compared with the actual aorta. Starting with the healthy aorta, $\sigma^2_{PVA} = 4.16$, $\sigma^2_{Si} = 4.56$, $\sigma^2_{Actual} = 0.84$ followed by the aortic dissection $\sigma^2_{PVA} = 28.57$, $\sigma^2_{Si} = 91.97$, $\sigma^2_{Actual} = 11.13$, which is shown in Tab. 4.

## Ultrasound features

The low-fidelity simulators of the healthy aorta and aortic dissection were immersed in the agarose, as shown in Fig. 4. The anatomical evaluations of both healthy AAo and aortic dissection simulator were conducted through the US in the UTM ultrasound clinic. The US image visualised the aorta with the echoic that exists around the simulator due to the agarose. The simulator itself was able to reflect the image and reveal the anatomically ascending area of the aorta in the transverse and long-axis views.

The PVA synthesised simulator was detected in the transverse view and shown in the monitor; then the measurement of the diameter ($d$) and wall thickness ($t$) was performed by using clipper tools. The diameter of the healthy AAo synthesised by PVA showed $d = 19.7$ mm – $20.2$ mm and $t = 2.7$ mm. In addition, the diameter of the AD simulator showed $d = 30$ mm – $43.5$ mm and $t = 1.7$ mm. Referring to the simulator synthesised by Si, the images showed the healthy aorta had a diameter $d = 23.5$ mm – $26.6$ mm and $t = 3$ mm. Moreover, the AD simulator showed $d = 31$ mm – $33.6$ mm and $t = 1.6$ mm.

**Tab. 1.** Surface texture morphology of PVA and silicone simulators in SEM test (healthy AAo and AD compared to the actual aorta)

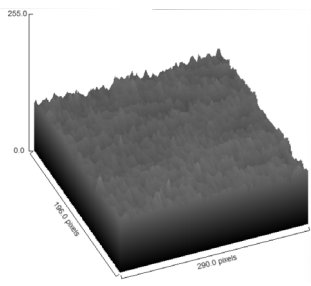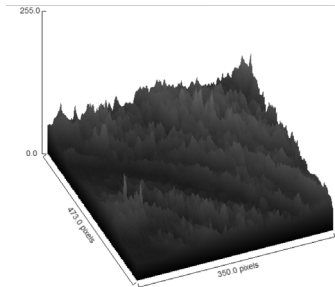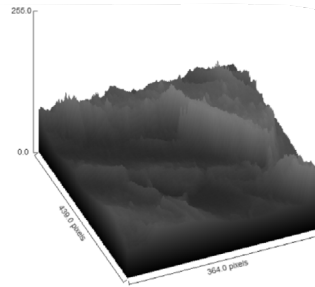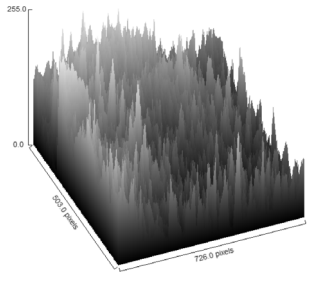| | Simulator synthesised by PVA | Simulator synthesised by silicone | Actual aorta[17,24] |
|---|---|---|---|
| Healthy aorta |  |  |  |
| Aortic dissection |  |  |  |
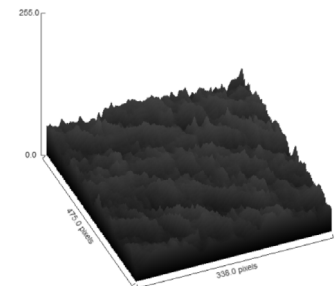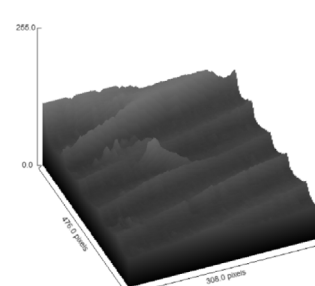
## Echogenicity

The B-mode image of the US was analysed to identify the echogenicity of the intimal flap. In the transverse and long-axis views of the ultrasound image, the AD simulator was able to visualise the intimal flap due to the dissection and the false lumen, as shown with the arrow in Tab. 5. The intimal flap echogenicity was then measured using imageJ to calculate the average grey value ($\mu$) of the intimal flap (IF) and average grey in the false lumen (FL)

**Tab. 2.** Root mean square (RMS) value obtained from (Rq) in imageJ between the healthy aorta (AAo) and AD simulator synthesised from PVA and silicone

| Root Mean Square (RMS) | PVA | Silicone | Actual aorta |
|---|---|---|---|
| Healthy aorta (AAo) | 10.26 | 23.07 | 13.11 |
| Aortic dissection (AD) | 20.28 | 33.8 | 38.83 |
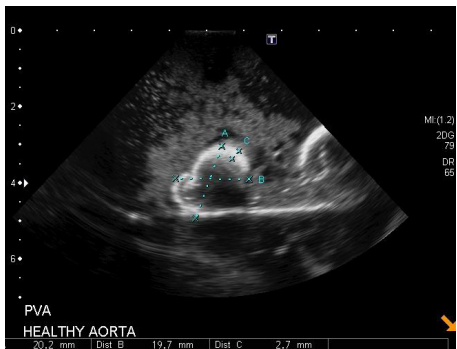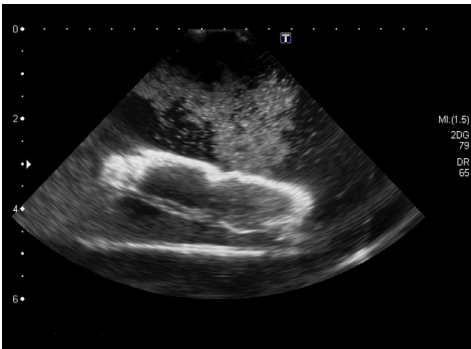
**Tab. 3.** 3D surface plot of SEM images analysed with imageJ between the healthy AAo and AD simulator (PVA and silicone) and the actual aorta

| | Simulator synthesised by PVA | Simulator synthesised by silicone | Actual aorta |
|---|---|---|---|
| Healthy AAo |  |  |  |
| Aortic dissection |  |  |  |

**Tab. 4.** Surface plot of grey value in each pixel obtained by imageJ between the healthy AAo and aortic dissection, compared by simulators and the actual aorta
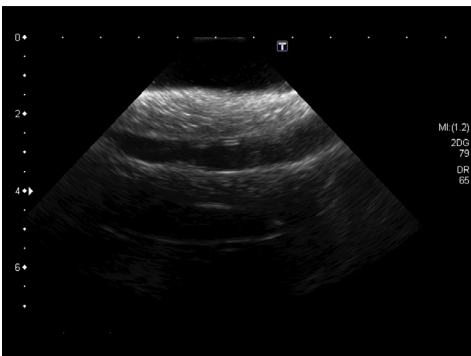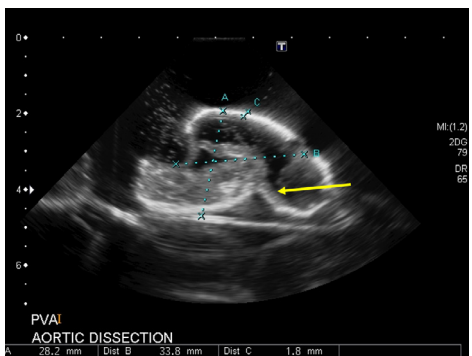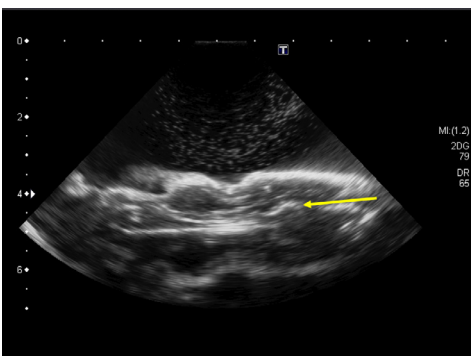
|  | PVA (healthy AAo) | PVA (aortic dissection) | Si (healthy AAo) | Si (aortic dissection) | Actual (healthy AAo) | Actual (aortic dissection) |
|---|---|---|---|---|---|---|
| **Min** | 40.46 | 41.78 | 58.23 | 60.18 | 92.89 | 64.35 |
| **Max** | 52.01 | 59.62 | 66.78 | 91.54 | 98.23 | 109.59 |
| $\sigma$ | 2.04 | 5.35 | 2.14 | 9.59 | 0.92 | 13.68 |
| $\sigma^2$ | 4.16 | 28.57 | 4.56 | 91.97 | 0.84 | 187.36 |

**Tab. 5.** Ultrasound images of the healthy aorta and aortic dissection simulators (PVA and silicone) and the actual aorta (comparison of short-axis and longitudinal views)

| | Short-axis view | Longitudinal view |
|---|---|---|
| **Healthy aorta of PVA** |  $d_A = 20.2$ mm, $d_B = 19.7$ mm, $t_C = 2.7$ mm |  |
| **Healthy aorta of silicone** |  $d_A = 22.4$ mm, $d_B = 26.9$ mm, $t_C = 23$ mm |  |
| **Aortic dissection of PVA** |  $d_A = 28.2$ mm, $d_B = 33.8$ mm, $t_C = 1.8$ mm |  |

| | Short-axis view | Longitudinal view |
|---|---|---|
| **Aortic dissection of silicone** |  $d_A = 31.0$ mm, $d_B = 33.6$ mm, $t_C = 1.6$ mm |  |
| **Actual aortic dissection image**[25] |  $d_A = 31.0$ mm, $d_B = 31.5$ mm, $t_C = 0.64–2.31$ mm |  |
| **Notes** | In the short-axis view, the diameter of the aorta is indicated by the letters A and B, while its thickness by the letter C. The arrow marks the intimal flap in the AD images. In the long-axis view, the healthy aorta images show the ascending aorta in its normal condition with no flap, whereas the AD indicated by the arrow shows the presence of the flap. | |

of the dissected area as the echogenicity index (*EI*). The AD simulator synthesised by PVA showed $\mu_{IF} = 170.89$ and $EI_{FL} = 85.27$, while the AD simulator synthesised by Si showed $\mu_{IF} = 99.36$, and $EI_{FL} = 77.84$. Statistical analysis of the Fisher's exact value between ($\mu_{IF}$, $EI_{FL}$) and (PVA, Si) showed 0.0264, which is below the *p* value ($p < 0.05$). The result of the echogenicity index between PVA and silicone summarises in Tab.**6**.

## Discussion

The physical characteristics of the simulator's surface structure imitated the ascending area of the human tissue. It was the results of printing a 3D mould that was designed based on the CT scan image obtained from the AD's patient. The aortic dissection simulator appeared physically rougher on the separation surface than the healthy aorta simulator. To extract information about the surface structure and different roughness of the healthy aorta and the AD simulator, the RMS value was measured. The total surface roughness from the RMS value for the PVA-based AD simulator was ($Rq_{AD} = 20.28 > Rq_{HealthyAorta} = 10.26$) and for the silicone-based AD simulator it was ($Rq_{AD} = 33.8 > Rq_{HealthyAorta} = 23.07$), indicating the AD high rough surface than the healthy aorta simulator, respectively. The

**Tab. 6.** Average grey value of the intimal flap ($\mu_{IF}$) and echogenicity index of false lumen ($EI_{FL}$) obtained from imageJ of AD simulator ultrasound image between PVA and silicone

| | Healthy aorta | |
|---|---|---|
| **Simulator** | **Average Grey Value** ($\mu_{IF}$) | **Echogenicity Index** ($EI_{FL}$) |
| **PVA** | 170.89 | 85.27 |
| **Silicone** | 99.36 | 77.84 |
| | | $p < 0.05$ |

surface plot showed that the variance of the healthy aorta ($\sigma^2_{PVA} = 4.16$, $\sigma^2_{Si} = 4.56$, $\sigma^2_{Actual} = 0.84$) was lower than of the aortic dissection ($\sigma^2_{PVA} = 28.57$, $\sigma^2_{Si} = 91.57$, $\sigma^2_{Actual} = 11.13$), indicating that the distribution of grey values in the healthy simulator aorta was more clumped and spreading of light intensity in dissection. It is attributed to the rough and uneven surface texture of the affected area caused by the disease.

The material used in this study has an impact on the echogenicity of ultrasound image. For example, PVA exhibits a high level of
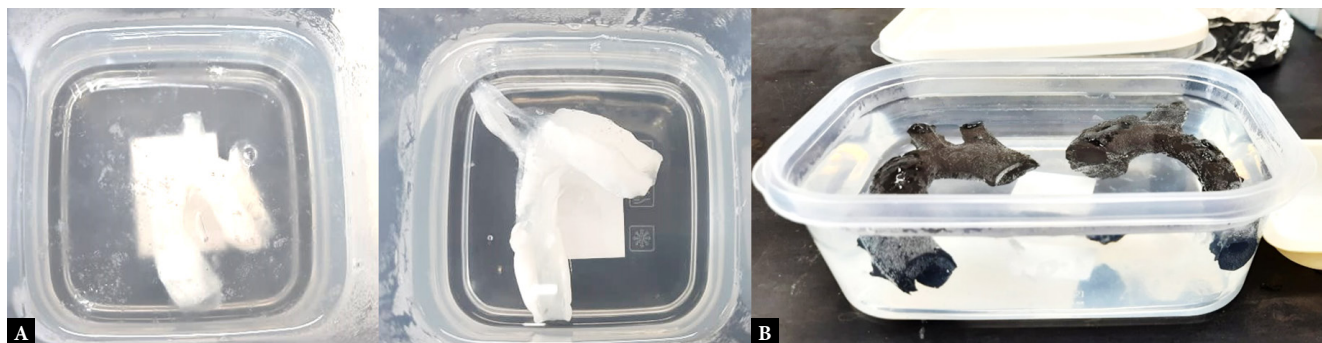
**Fig. 4**. *Low-fidelity simulators immersed in agarose* **A.** *Healthy aorta (left), aortic dissection synthesised from PVA (right);* **B.** *Healthy aorta (left), aortic dissection synthesised from silicone (right)*

hydrolysis and aluminium oxide acts as a scatterer, which helps the simulator to reflect during the ultrasound assessment[12]. The coated bubbles inside polymers that make small air pockets inside result in the echogenicity in the ultrasound image. In addition, the freeze-thaw method applied, which causes the presence of dissolved gas, also generates echogenicity by trapping air in the bilayer[20]. The echogenicity of Si allows the simulator to be identified in US images due to the presence of an additive material (graphite), serving as a scatterer agent in Si[21]. Additionally, the higher echogenicity expected for a soft-tissue which has a rougher or varied dimple surface rather than a flat surface[22].

During the US examination, the differences between the healthy AAo and AD simulators were able to be visualised. A comparison of the diameter and wall thickness between the simulator and the actual aorta is shown in the Tab. 4. The healthy adult aorta has $d = 2.5$ mm – 35 mm, $t = 1$ mm – 3 mm, and AD has $d = 31.5$ mm (exceeding 50%) and wall thickness $t = 0.64$ mm – 2.31 mm within the actual tissue[23,24,25]. The wide diameter of AD in comparison with the healthy AAo in PVA ($d_{AD} = 28.2$ mm $> d_{AAo} = 20.2$ mm) and Si ($d_{AD} = 31.0$ mm $> d_{AAo} = 22.4$ mm), the wall thickness of AD appeared thinner than the healthy Ao in PVA ($t_{AD} = 1.7$ mm $< t_{AAo} = 2.7$ mm) and Si ($t_{AD} = 1.6$ mm $< t_{AAo} = 3$ mm). These findings of simulator measurements indicated comparable measures with the real aorta in terms of diameter and wall thickness under PoCUS testing which was conducted at the ultrasound clinic at the university. The US images were quantitatively measured by comparing the grey value with the echogenicity index. The result of flap measurement was greater than the false lumen ($\mu_{IF} = 170.89 > EI_{FL} = 85.27$) in PVA and Si ($\mu_{IF} = 99.36 > EI_{FL} = 77.84$). The average grey value resulted in a higher value for the intimal flap than the average grey value representing the separation of the wall of the aorta, resulting in hyperechogenicity of the intimal flap. This study found a statistically significant difference between the intimal flap and the false lumen. The findings support the utility of echogenicity testing in the AD simulator (PVA and Si) for determining the presence of the intimal flap during US assessment. Hence, the anatomy of AD was able to be visualised by the simulator in the ultrasound images by measuring the diameter, wall thickness, and identification of the intimal flap that exists due to the tear and creates false lumen.

## Conclusions

For the purpose of the reported study, we created in-house designed aortic dissection and healthy aorta simulators and tested them to determine whether they exhibited realistic anatomical sonographic features and thus had a potential for future applications in PoCUS training tools. The results from the US assessment of the synthesised simulators were comparable to the open source-retrieved US images and measurements done in actual patients. The AD simulators were able to replicate the intimal flap, which indicates hyperechoic properties that can be seen and differentiated between the healthy aorta and aortic dissection by using PoCUS. As a result, based on simulator characteristics that are relevant to the actual tissue, emergency medical physicians are able to plan and simulate actions that will be performed on patients using the simulator, as well as provide training tools for them to practise.

## Conflict of interest

*The authors declare that there are no competing interests.*

## Author contributions

*Original concept of study: RHA. Writing of manuscript: MR, YTL. Analysis and interpretation of data: MR, RHA, MIS. Final approval of manuscript: RHA. Collection, recording and/or compilation of data: MR, YWH. Critical review of manuscript: RHA.*

## References

1. Levy D, Goyal A, Grigorova Y, Farci F, Le JK: Aortic Dissection. In: StatPearls. Treasure Island (FL), StatPearls Publishing 2023. Available from: https://www.ncbi.nlm.nih.gov/books/NBK441963/.

2. Tan GJS, Khoo PLZ, Sailesh MK, Chan KMJ: A review of aortic disease research in Malaysia. Med J Malaysia 2019; 74: 67–78.

3. Salameh MJ, Ratchford EV: Aortic dissection. Vasc Med 2016; 21: 276–280. doi: 10.1177/1358863X16632898.

4. Pape LA, Awais M, Woznicki EM, Suzuki T, Trimarchi S, Evangelista A *et al.*: Presentation, diagnosis, and outcomes of acute aortic dissection. J Am Coll Cardiol 2015; 66: 350–358. doi: 10.1016/j.jacc.2015.05.029.

5. Hebballi R, Swanevelder J: Diagnosis and management of aortic dissection. Cont Educ Anaesth Crit Care Pain 2009; 9: 14–18. doi: 10.1093/bjaceaccp/mkn044.

6. Hashim A, Tahir MJ, Ullah I, Asghar MS, Siddiqi H, Yousaf Z: The utility of point of care ultrasonography (POCUS). Ann Med Surg 2021; 71: 102982. doi: 10.1016/j.amsu.2021.102982.

7. Iserson KV, Devi Jagjit S, Doodnauth B: Ultrasound diagnosis of dissecting thoracic aortic aneurysms: procedure with a handheld device and a video-illustrated case. Trop Doct 2021; 51: 10–15. doi: 10.1177/0049475520959906.

8. Lewiss RE, Hoffmann B, Beaulieu Y, Phelan MB: Point-of-care ultrasound education. J Ultrasound Med 2014; 33: 27–32. doi: 10.7863/ultra.33.1.27.

9. Lapkin S, Fernandez R, Levett-Jones T, Bellchambers H: The effectiveness of using human patient simulation manikins in the teaching of clinical reasoning skills to undergraduate nursing students: a systematic review. JBI Libr Syst Rev 2010; 8: 661–694. doi: 10.11124/01938924-201008160-00001.

10. Fresiello L, Ferrari G, Di Molfetta A, Zieliński K, Tzallas A, Jacobs S *et al.*: A cardiovascular simulator tailored for training and clinical uses. J Biomed Inform 2015; 57: 100–112. doi: 10.1016/j.jbi.2015.07.004.

11. Rajeshkumar G, Vishnupriyan R, Selvadeepak S: Tissue mimicking material an idealized tissue model for clinical applications: a review. Mat Today Proc 2020; 22: 2696–2703. doi: 10.1016/j.matpr.2020.03.400.

12. Cournane S, Cannon L, Browne JE, Fagan AJ: Assessment of the accuracy of an ultrasound elastography liver scanning system using a PVA-cryogel phantom with optimal acoustic and mechanical properties. Phys Med Biol 2010; 55: 5965–5983. doi: 10.1088/0031-9155/55/19/022.

13. Tarique J, Sapuan SM, Khalina A: Effect of glycerol plasticizer loading on the physical, mechanical, thermal, and barrier properties of arrowroot (Maranta arundinacea) starch biopolymers. Sci Rep 2010, 11: 13900. doi: 10.1038/s41598-021-93094-y.

14. Pacioni A, Carbone M, Freschi C, Viglialoro R, Ferrari V, Ferrari M: Patient-specific ultrasound liver phantom: materials and fabrication method. Int J Comput Assist Radiol Surg 2014; 10: 1065–1075. doi: 10.1007/s11548-014-1120-y.

15. McNaughtion A: Measuring surface roughness using confocal microscopy and ImageJ (or Fiji variant). In: Otago Cente for Confocal Microscopy. 2017. Available from: https://www.otago.ac.nz/omni/otago684709.pdf.

16. Barthel K: 3D-data representation with ImageJ. 2006. Available from: https://www.researchgate.net/publication/215458973_3D-Data_Representation_with_ImageJ.

17. Pasta S, Phillippi JA, Gleason TG, Vorp DA: Effect of aneurysm on the mechanical dissection properties of the human ascending thoracic aorta. J Thorac Cardiovasc Surg 2012; 143: 460–467. doi: 10.1016/j.jtcvs.2011.07.058.

18. Elefteriades JA, Mukherjee SK, Mojibian H: Discrepancies in measurement of the thoracic aorta. J Am Coll Cardiol 2020; 76: 201–217. doi: 10.1016/j.jacc.2020.03.084.

19. Sendić G: Aorta. In: Kenhub. 2023. Available from: https://www.kenhub.com/en/library/anatomy/aorta.

20. Stecco A, Pirri C, De Caro R, Raghavan P: Stiffness and echogenicity: development of a stiffness-echogenicity matrix for clinical problem solving. Europ J Transl Myol 2019; 29: 8476. doi: 10.4081/ejtm.2019.8476.

21. Xia L, Karandish F, Kumar KN, Froberg J, Kulkarni P, Gange KN *et al.*: Acoustic characterization of Echogenic polymersomes prepared from amphiphilic block copolymers. Ultrasound Med Biol 2018; 44: 447–457. doi: 10.1016/j.ultrasmedbio.2017.10.011.

22. Markham SK, Mani A, Bauer J, Silien C, Tofail SAM: Surface texturing design to enhance echogenicity of biopsy needles during endoscopic ultrasound imaging. Ultrasound Med Biol 2020; 46: 2453–2463. doi: 10.1016/j.ultrasmedbio.2020.04.034.

23. Van Puyvelde J, Verbeken E, Verbrugghe P, Herijgers P, Meuris B: Aortic wall thickness in patients with ascending aortic aneurysm versus acute aortic dissection. Europ J Cardiothorac Surg 2016; 49: 756–762. doi: 10.1093/ejcts/ezv197.

24. Schmitto JD, Popov AF, Coskun KO, Friedrich M, Sossalla S, Didilis V: Morphological investigations of type A aortic dissection. Ann Thorac Cardiovasc Surg 2010; 16: 331–334.

25. Henderson S: Aortic dissection diagnosed by ultrasound. In: The Western Journal of Emergency Medicine 2014. Available from: http://westjem.com/articles/aortic-dissection-diagnosed-by-ultrasound.html.